

Published in final edited form as:

Nat Med. 2008 August ; 14(8): 843–848. doi:10.1038/nm1788.

Reversal of learning deficits in a *Tsc2*^{+/-} mouse model of tuberous sclerosis

Dan Ehninger¹, Sangyeul Han², Carrie Shilyansky¹, Yu Zhou¹, Weidong Li¹, David J Kwiatkowski³, Vijaya Ramesh², and Alcino J Silva¹

¹ Departments of Neurobiology, Psychiatry & Biobehavioral Sciences, Psychology and the Brain Research Institute, University of California, Los Angeles, 695 Charles E. Young Drive South, Los Angeles, California 90095, USA

² Center for Human Genetic Research, Massachusetts General Hospital, Harvard Medical School, Richard B. Simches Research Center, 185 Cambridge Street, Boston, Massachusetts 02114, USA

³ Genetics Laboratory, Division of Translational Medicine, Brigham and Women's Hospital, Harvard Medical School, 221 Longwood Avenue, Boston, Massachusetts 02115, USA

Abstract

Tuberous sclerosis is a single-gene disorder caused by heterozygous mutations in the *TSC1* (9q34) or *TSC2* (16p13.3) gene^{1,2} and is frequently associated with mental retardation, autism and epilepsy. Even individuals with tuberous sclerosis and a normal intelligence quotient (approximately 50%)^{3–5} are commonly affected with specific neuropsychological problems, including long-term and working memory deficits^{6,7}. Here we report that mice with a heterozygous, inactivating mutation in the *Tsc2* gene (*Tsc2*^{+/-} mice)⁸ show deficits in learning and memory. Cognitive deficits in *Tsc2*^{+/-} mice emerged in the absence of neuropathology and seizures, demonstrating that other disease mechanisms are involved^{5,9–11}. We show that hyperactive hippocampal mammalian target of rapamycin (mTOR) signaling led to abnormal long-term potentiation in the CA1 region of the hippocampus and consequently to deficits in hippocampal-dependent learning. These deficits included impairments in two spatial learning tasks and in contextual discrimination. Notably, we show that a brief treatment with the mTOR inhibitor rapamycin in adult mice rescues not only the synaptic plasticity, but also the behavioral deficits in this animal model of tuberous sclerosis. The results presented here reveal a biological basis for some of the cognitive deficits associated with tuberous sclerosis, and they show that treatment with mTOR antagonists ameliorates cognitive dysfunction in a mouse model of this disorder.

To address the mechanisms of tuberous sclerosis–related cognitive deficits, we first determined whether *Tsc2*^{+/-} mice had learning and memory impairments. Because the tuberous sclerosis genes are highly expressed in adult brain, including hippocampus¹², and hippocampal dysfunction could contribute to the tuberous sclerosis phenotype, we studied spatial learning

Correspondence should be addressed to A.J.S. (silvaa@mednet.ucla.edu).

Note: Supplementary information is available on the Nature Medicine website.

AUTHOR CONTRIBUTIONS

D.E. and A.J.S. conceptualized the research; D.E. performed behavioral experiments and the *Tsc1*^{cc}– α CaMKII–Cre study (Figs. 1, 3 and 4; Supplementary Figs. 3, 4, 6; Supplementary Table 1); D.E., C.S. and Y.Z. contributed to slice physiology experiments (Fig. 2; Supplementary Figs. 2 and 5); S.H., V.R., D.E. and W.L. contributed to western blot experiments (Supplementary Fig. 1); D.E. analyzed the data; D.J.K. provided *Tsc1*^{cc} and *Tsc2*^{+/-} founders for the mouse colony; D.E. and A.J.S. wrote the manuscript.

Published online at <http://www.nature.com/naturemedicine/>

Reprints and permissions information is available online at <http://npg.nature.com/reprintsandpermissions/>

in the Morris water maze. Initially, mice were tested in a hippocampus-dependent version of the Morris water maze, in which they use distal spatial cues to navigate and locate a hidden escape platform (Fig. 1a). To assess whether the mice had learned the position of the escape platform, we gave a probe trial (during which the platform was removed from the pool) at the end of training. Probe trial data show that searches from wild-type (WT) mice were more selective than those from *Tsc2*^{+/-} mice, indicating spatial learning deficits in these mutants (Fig. 1a). Studies with the hippocampus-independent, visible version of the water maze (Supplementary Table 1 online) revealed no differences between *Tsc2*^{+/-} mice and WT controls, suggesting that motivational, perceptual or motor differences are unlikely to account for the observed spatial learning phenotype. Moreover, additional behavioral characterization revealed normal motor skills, anxiety, exploratory activity and social approach behavior in *Tsc2*^{+/-} mice (Supplementary Table 1). These results show that spatial learning in the Morris water maze was poorer in *Tsc2*^{+/-} mice than in WT controls.

Because humans affected by tuberous sclerosis may have working memory deficits⁷, and because the hippocampus can contribute to working memory¹³, we next tested *Tsc2*^{+/-} mice on a hippocampus-dependent win-shift version of the eight-arm radial maze (Fig. 1b), a commonly used working memory task¹⁴. In this task, food-deprived mice were first allowed to retrieve food pellets from four accessible arms of an eight-arm maze (phase A). After a retention interval of 2 min, mice were brought back to the maze (phase B) and given access to all eight arms (only the four previously blocked arms were now baited). In this task, mice can commit two types of errors: within-phase errors are committed when mice enter an arm previously visited in the same phase, and across-phase errors are committed when mice enter an arm in phase B that they had already visited in phase A. Although *Tsc2*^{+/-} mice did not differ from wild-type controls in the number of within-phase errors (data not shown), they did make significantly more across-phase errors ($P = 0.0364$; Fig. 1b). This pattern of errors in the radial arm maze is consistent with deficits in hippocampal function^{13,14}.

Discriminating between similar contexts is known to also depend on hippocampal function¹⁵. Mice were trained in context conditioning with three 0.75-mA shocks and tested in the training context or a novel context (detailed in Methods). WT mice showed clear discrimination between both contexts (Fig. 1c). The freezing responses of *Tsc2*^{+/-} mice, however, lacked context specificity, confirming hippocampal dysfunction in these mutants¹⁵.

The behavioral data presented above demonstrate deficits in three distinct hippocampal-dependent tasks. Therefore, next we tested whether TSC protein levels and TSC-mTOR signaling were altered in the hippocampus of *Tsc2*^{+/-} mice. Although genetic analyses of tuberous sclerosis have revealed a large number of different mutations in the tuberous sclerosis genes¹⁶, the majority results in premature truncation of TSC proteins. Nevertheless, there are also large deletions and rearrangements that encompass the whole *TSC1* or *TSC2* gene. In the *Tsc2*^{+/-} mouse model, the *Tsc2* gene is disrupted by insertion of a selection cassette in its second coding exon⁸. We found that tuberin (Tsc2) abundance in whole hippocampal extracts of *Tsc2*^{+/-} mice was reduced to about 75% of WT levels, whereas hamartin (Tsc1) abundance was unchanged (Supplementary Fig. 1 online). Tuberin is a GTPase-activating protein that regulates the small G protein Rheb, a strong activator of mTOR¹⁷. Consequently, loss of hippocampal tuberin should result in disinhibition of mTOR signaling. We determined the phosphorylation status of the S6 ribosomal protein at Ser235 and Ser236 in whole hippocampal extracts, as phosphorylation at these sites is regulated by the mTOR pathway and correlates with translational rates. We found higher levels of phosphorylated S6 (p-S6, on Ser235 and Ser236) in hippocampi of *Tsc2*^{+/-} mice than in WT controls (Supplementary Fig. 1), indicating that mTOR signaling was disinhibited in *Tsc2*^{+/-} hippocampus, a result consistent with the inhibitory role of TSC proteins in mTOR signaling¹⁷.

Hippocampal activity-dependent synaptic plasticity such as long-term potentiation (LTP) has a major role in learning processes. To determine whether synaptic plasticity is altered in *Tsc2*^{+/-} mice, we performed standard extracellular field recordings in acute hippocampal slices from adult *Tsc2*^{+/-} mice and WT controls. Basal synaptic transmission, paired-pulse facilitation and early-phase LTP (E-LTP) at the Schaffer collateral-CA1 synapse were normal in *Tsc2*^{+/-} mice (Supplementary Fig. 2 online), demonstrating that several aspects of synaptic function were normal in these mice.

As mTOR signaling plays a part in the regulation of the late-phase of LTP (L-LTP)¹⁸, we next studied this form of synaptic plasticity. Because we detected disinhibited mTOR signaling, we started by using an E-LTP induction paradigm (100-Hz, 1-s tetanus) and recorded responses for 4 h. As expected, this paradigm caused decaying LTP in WT slices but was sufficient to induce stable L-LTP in *Tsc2*^{+/-} slices (Fig. 2). The lower threshold for L-LTP induction in the mutants could cause a lower threshold for memory consolidation. This could lead to inappropriate storage of unrelated or unprocessed information, thus resulting in learning impairments.

The studies presented above show that *Tsc2*^{+/-} mice are a useful model of some of the learning and memory deficits associated with tuberous sclerosis, and they suggest that enhanced mTOR signaling leads to abnormal L-LTP thresholds that account for these deficits. To test this hypothesis, we next determined whether rapamycin could rescue the learning and L-LTP abnormalities of *Tsc2*^{+/-} mice. We suppressed mTOR signaling by administering rapamycin before learning. A treatment regimen (described in Methods) was established that effectively reduced hippocampal p-S6 (on Ser235 and Ser236) abundance (Supplementary Fig. 1) and did not measurably affect behavior in WT mice (Supplementary Fig. 3 online). After rapamycin treatment, mice were trained and tested in context discrimination as described above. Rapamycin did not affect context discrimination in WT controls; strikingly, however, this treatment reversed the context discrimination deficits of *Tsc2*^{+/-} mice (Fig. 3a).

Next, we tested whether rapamycin treatment could also ameliorate the learning deficits of *Tsc2*^{+/-} mice in the Morris water maze (Fig. 3b). Before daily training, we treated WT and mutant mice with rapamycin or vehicle and assessed spatial learning with a probe trial after completion of training. Measurements of quadrant occupancy and target crossings indicated selective searching in WT mice on rapamycin and vehicle, but not in vehicle-treated *Tsc2*^{+/-} mice (Fig. 3b). Notably, rapamycin-treated *Tsc2*^{+/-} mice showed selective searching, as shown by their preference for the target quadrant and target position (Fig. 3b). Collectively, these results show that the learning impairments described for *Tsc2*^{+/-} mice are caused by enhanced mTOR signaling and that a brief pharmacological treatment with rapamycin can reverse these deficits in adult mice. Unlike rapamycin, the 3-hydroxy-3-methyl-glutaryl-CoA (HMG-CoA) reductase inhibitor lovastatin (which rescued learning deficits in a mouse model of neurofibromatosis type 1; see Supplementary Fig. 4 online) did not rescue the spatial learning deficits of *Tsc2*^{+/-} mice (Supplementary Fig. 4), a result that attests to the specificity of the rapamycin effects.

To explore the hypothesis that the change in L-LTP thresholds contributes to the learning deficits of *Tsc2*^{+/-} mice, we next tested whether rapamycin also reverses the abnormal LTP in *Tsc2*^{+/-} mice. As above, LTP was induced with a 100-Hz, 1-s tetanus and responses were recorded for 4 h (slices were perfused with rapamycin or vehicle). Vehicle-treated *Tsc2*^{+/-} slices showed stable L-LTP after induction with the E-LTP stimulation paradigm, whereas LTP in vehicle-treated WT slices decayed throughout recording (Supplementary Fig. 5 online). As expected, rapamycin did not affect the E-LTP of WT slices; however, this treatment reversed the abnormal induction of L-LTP in *Tsc2*^{+/-} slices (Supplementary Fig. 5). These findings

indicate that treatment with rapamycin rescues the abnormal L-LTP of *Tsc2*^{+/-} mutants, just as it rescues their learning deficits, and that enhanced mTOR signaling causes both phenotypes.

To test the efficacy of rapamycin in modulating other tuberous sclerosis brain phenotypes, we studied a homozygous conditional deletion of *Tsc1* in neurons of the postnatal forebrain: floxed *Tsc1* mice (*Tsc1*^{cc})¹⁹ were crossed with mice expressing Cre recombinase under the control of the promoter for α CaMKII (α CaMKII-Cre)²⁰. Not unexpectedly, the resulting mice had a much more profoundly impaired phenotype than heterozygous *Tsc2*^{+/-} mice (Fig. 4, Supplementary Fig. 6 online, Supplementary Table 1 and data not shown). The majority of *Tsc1*^{cc}- α CaMKII-Cre mice died within the first postnatal weeks (data not shown). Rare surviving *Tsc1*^{cc}- α CaMKII-Cre mice (~4% of what would be predicted by Mendelian ratios) developed extreme macroencephaly, with brain weights being ~2.5 times that of control brains (Supplementary Fig. 6). Brain enlargement was largely due to massive neuronal hypertrophy and was accompanied by astrogliosis (Supplementary Fig. 6). *Tsc1*^{cc}- α CaMKII-Cre mice showed a pathological hindlimb clasp reflex (Supplementary Fig. 6) and were severely hypoactive.

Rapamycin treatment substantially increased survival of *Tsc1*^{cc}- α CaMKII-Cre mice (Fig. 4a; to ~70% of what would be expected by Mendelian ratios), decreased brain enlargement (Fig. 4b) and improved the neurological findings in *Tsc1*^{cc}- α CaMKII-Cre mice (Fig. 4c,d). These data attest to the efficacy of rapamycin in modulating brain phenotypes associated with mutations in *Tsc* genes. Our findings suggest that rapamycin may be able to ameliorate putative developmental deficits, potentially contributing to the profound cognitive abnormalities present in a subset of individuals with tuberous sclerosis⁴. Of note, a null mutation of the *Pten* gene caused some of the same phenotypes described for the *Tsc1*^{cc}- α CaMKII-Cre mice, and mTOR antagonists also rescued these phenotypes²¹. This result is consistent with the role of PTEN as an upstream regulator of the TSC-mTOR pathway.

The neurocognitive phenotype associated with tuberous sclerosis is complex. The distribution of intelligence quotient (IQ) scores of individuals with tuberous sclerosis indicates the existence of two distinct subpopulations^{3,4}: a profoundly impaired group with severe mental retardation (30%) and a group with normally distributed IQs with a slight reduction in mean IQ (70%). This group is affected by certain neuropsychological impairments, such as specific learning disabilities and memory problems⁵⁻⁷. Similarly, the *Tsc2*^{+/-} mutation in mice also resulted in a specific behavioral phenotype: it disrupted hippocampal-dependent learning while leaving most other tested behaviors unaffected (Supplementary Table 1). It will be useful to determine whether individuals with tuberous sclerosis also show abnormal hippocampal function. Deficient context discrimination is a key component of hippocampal dysfunction in *Tsc2*^{+/-} mice. It is possible that deficits in contextual discrimination lead to overgeneralized fear and contribute to anxiety disorders, frequently encountered in individuals with tuberous sclerosis²². As rapamycin rescued these cognitive deficits in mice, it may also ameliorate cognitive impairments in individuals with tuberous sclerosis. Nevertheless, even though our studies showed that rapamycin rescued phenotypes other than spatial learning deficits (that is, *Tsc1*^{cc}- α CaMKII-Cre phenotypes), it is unclear whether rapamycin will reverse cognitive deficits caused by cerebral malformations or infantile spasms^{23,24}.

Consistent with a recent study¹¹, our studies show that tuberous sclerosis-related cognitive deficits emerged in the absence of spontaneous seizures and neuropathology, suggesting that other mechanisms are involved in causing cognitive dysfunction. Indeed, we found that increased mTOR signaling changed the induction of the late phase of LTP, a finding that most likely accounts for the learning and memory deficits in the *Tsc2*^{+/-} mutants. Notably, our results are consistent with previous findings that implicated TSC-mTOR signaling in synaptic plasticity. First, the TSC-mTOR pathway regulates the local translation of specific proteins

known to have crucial roles in LTP^{18,25}. Second, *Tsc1*^{-/-} hippocampal neurons were shown to have morphological and functional synaptic abnormalities²⁶. Third, changes in the induction of the late phase of LTP as well as learning deficits have also been reported in mice lacking 4E-BP2, which also show increased mTOR-dependent translational initiation²⁷. Altogether, these results strongly suggest that the change in L-LTP that we found accounts for the learning deficits of *Tsc2*^{+/-} mice.

A key finding reported here is that a brief rapamycin treatment of adult *Tsc2*^{+/-} mice rescued not only their physiological abnormalities, but, more importantly, their learning and memory deficits. Our results also suggest that there is an optimal range for translational activation during learning and memory processes: decreases in translation (for example, with high doses of rapamycin; Supplementary Fig. 3)²⁸ as well as hyperactivation of translation (for example, by the *Tsc2*^{+/-} mutation) disrupt learning and memory. Excessive mTOR-dependent neuronal protein synthesis is also involved in other neurogenetic syndromes linked to mental retardation and autism^{29,30}. Identifying the crucial mechanisms disrupted by changes in translation will not only provide insights into the role of this process in learning and memory, but also may inform treatment development.

A recent study reported hippocampal-dependent learning deficits in *Tsc1*^{+/-} mice¹¹. Unlike *Tsc2*^{+/-} mutants, however, *Tsc1*^{+/-} mice also show abnormal social behavior. This difference could be due either to the specific gene disrupted or to the genetic background. Because there is a close functional interaction between the Tsc1 and Tsc2 proteins, it is more likely that genetic background^{8,11} accounts for the differences in social behavior. Genetic background could also be responsible for the high variability of the human tuberous sclerosis phenotype⁵. Another major model of tuberous sclerosis, the Eker rat, shows synaptic plasticity abnormalities, including LTP and LTD deficits¹⁰. Of note, these rats show many features associated with tuberous sclerosis, but no behavioral deficits⁹. Instead, behavioral analysis reveals enhancements in episodic-like memory⁹, a result consistent with the idea that modifier genes in the genetic background influence the expressivity of tuberous sclerosis phenotypes^{5,8,11}.

In summary, our results show that *Tsc2*^{+/-} mice model some of the neurocognitive deficits associated with tuberous sclerosis. As predicted previously⁵, we found that treatment with rapamycin in adult mice can reverse these deficits. Contrary to prevailing hypotheses^{23,24}, but in agreement with a recent study¹¹ and earlier predictions^{5,9,10}, our data show that tuberous sclerosis-related cognitive deficits are not necessarily the consequence of neuroanatomical abnormalities (that is, tubers) or seizures. Thus, it is possible that abnormalities in mTOR signaling and the associated physiological phenotypes (that is, abnormal synaptic plasticity) have a key role in some of the neurocognitive deficits associated with tuberous sclerosis. Our studies reveal that disinhibited mTOR signaling leads to a lower threshold for the induction of L-LTP, which probably underlies the behavioral deficits described here (for example, abnormal potentiation leading to inappropriate information storage). Altogether, these findings demonstrate the role of TSC-mTOR signaling in the modulation of L-LTP, learning and memory; they also raise the possibility that mTOR inhibitors could be used to treat cognitive deficits associated with tuberous sclerosis.

METHODS

Mice

Tsc2^{+/-} mice were generated as previously described⁸ (genetic background: C57BL/6NCrl). We used a balanced ratio of 3–6-month-old males and females. The generation of α CaMKII-Cre mice²⁰ (genetic background: C57BL/6NTac) and floxed *Tsc1* (*Tsc1*^c allele) mice¹⁹ (mixed genetic background composed of C57BL/6J, 129/SvJae, BALB/cJ) were also

previously described. For the generation of experimental mice, we crossed floxed *Tsc1* mice and α CaMKII-Cre transgenic mice. We show data separately for the *Tsc1^{cc}*- α CaMKII-Cre and *Tsc1⁺*- α CaMKII-Cre groups. When we found no significant differences between the remaining control groups, we pooled the data and show them as a single control group. All experiments were conducted blind to genotype and treatment condition. The Chancellor's Animal Research Committee at the University of California, Los Angeles approved the research protocols used here.

Rapamycin

We freshly dissolved rapamycin (LC Laboratories) in vehicle solution (specified below) before use. For the *Tsc2* *in vivo* experiments, we administered rapamycin intraperitoneally once daily at a dose of 5 mg/kg or 1 mg/kg (vehicle: 100% DMSO; DMSO dose: 2 ml/kg; volume of a single injection did not exceed 50 μ l). We gave injections (5 mg/kg) for 5 d before and on the day of fear conditioning (3 h before conditioning). In the water maze experiment, we injected mice daily 3 h before training (5 mg/kg or 1 mg/kg). For hippocampal slice physiology, we used rapamycin at a concentration of 200 nM; vehicle was 0.1% DMSO in oxygenated artificial CSF (ACSF). We continuously perfused slices with rapamycin (or vehicle) throughout the recording and for at least 30 min before tetanization. For the *Tsc1^{cc}*- α CaM-KII-Cre study, we injected rapamycin subcutaneously at a dose of 0.2 mg/kg per day (vehicle: 20% DMSO and 80% sterile physiological saline). We administered a single daily injection starting at postnatal day 1.

Behavior

For the hidden version of the Morris water maze, we trained mice with four training trials per day for 5 consecutive d. The escape platform was hidden 1 cm under the water surface in a constant location of the pool. We released mice into the pool from one of seven starting locations. Training trials ended when the mouse was on the platform or 60 s had elapsed, whichever came first. Mice remained for 15 s on the platform before they were removed from the pool. We gave training trials in blocks of two spaced about 90 min apart. We assessed spatial learning with a probe trial (during which the platform was removed from the pool) given after completion of training. We used ANOVAs and *t*-tests for analysis of data (quadrant occupancy, target crossings). After initial ANOVA analysis, we determined specificity of searching by comparing target quadrant measures to average measures of the other quadrants (paired *t*-test).

For the win-shift version of the eight-arm radial maze, we deprived mice of food until they reached 85% of their free-feeding body weight, shaped them to consume 20 mg food pellets and habituated them to the maze. On phase A of the task, we allowed mice to retrieve food pellets from four accessible arms of the eight-arm maze (access to the remaining arms was blocked). After a 2-min delay interval (in home cage), for phase B, we returned mice to the maze and allowed them to freely explore all eight arms. Food rewards were only located in the four previously blocked arms. We scored entries into arms that were visited on phase A as across-phase errors. We scored re-entries into arms that were visited earlier during the same phase as within-phase errors. Mice received one daily session for 8 consecutive d. We used one-way repeated-measures ANOVA with genotype as the between-subjects factor for statistical comparison of data (number of across-phase and within-phase errors).

For context fear conditioning, we fear-conditioned mice to the training context with three 0.75 mA shocks (2 s each). Training sessions were 5 min in duration. We assessed the conditioned fear response (as measure by the percentage of the time spent freezing during test, as scored by an experienced observer) to the training context 24 h after training (5 min session). To test for context specificity of the conditioned response, we tested a separate group of mice in a

novel context. This context was situated in another room with different distal cues and with some shared features (horizontal floor, ethanol scent, white background noise) with the training context, but was otherwise distinct (plastic instead of metal grid floor, angled instead of rectangular walls, red instead of white light, different distal spatial cues in room). We used *t*-tests to compare percentage time spent freezing to training and novel context for the different experimental conditions.

Hippocampal slice physiology

After killing mice with isoflurane, we extracted brains and completed slice preparation in ice-cold ACSF that was saturated with 95% O₂ and 5% CO₂ and contained (in mM): 120 NaCl, 20 NaHCO₃, 3.5 KCl, 2.5 CaCl₂, 1.3 MgSO₄ 1.25 NaH₂PO₄ and 10 D-glucose. We obtained 400- μ m sagittal slices with a Leica VT1000S vibratome and allowed them to recover at 23 °C for at least 70 min. We made recordings in a submerged chamber continuously perfused with oxygenated ACSF (29 °C) at a rate of 3 ml/min. We made extracellular recordings of field excitatory postsynaptic potentials (fEPSPs) with platinum-iridium electrodes in CA1 stratum radiatum. We stimulated Schaffer collaterals (pulse duration: 100 μ s) with bipolar platinum electrodes. For the input-output function, we stimulated slices with incrementally increasing current (from 10 μ A to 100 μ A in 10- μ A increments) and recorded fEPSP responses. For paired-pulse facilitation, we applied two pulses with different interstimulus intervals (10, 20, 50, 100, 200 or 400 ms). We induced LTP with theta burst stimulation (four bursts) or 1-s, 100-Hz stimulation. We determined initial fEPSP slopes and normalized them to the average baseline fEPSP slopes. We used repeated-measures ANOVAs on all responses after LTP induction and *t*-tests (on the average of the last 10 min of recording) for statistical analysis.

Statistical Analyses

Statistical tests (ANOVAs or *t*-tests) and parameters for data analysis were chosen *a priori* and are described in more detail in the sections above. $P < 0.05$ was considered statistically significant.

Additional methods

Detailed methodology is described in Supplementary Methods online.

Supplementary Material

Refer to Web version on PubMed Central for supplementary material.

Acknowledgements

The authors would like to thank B. Wiltgen, A. Matynia, Y.-S. Lee, R. Czajkowski, G. Ehninger and G. Kempermann for helpful comments on an earlier version of the manuscript and for valuable discussions, J.N. Crawley for helpful suggestions regarding the social interaction paradigm, M. Meredith-Steward for editing help, I. Röder for statistical advice and R. Chen and K. Cai for technical support. This work was supported by the following grants: Deutsche Forschungsgemeinschaft EH223/2-1 to D.E., US National Institutes of Health R01-NS38480 to A.J.S., US National Institutes of Health NS24279 and Autism Speaks to V.R.

References

1. European Chromosome 16 Tuberous Sclerosis Consortium. Identification and characterization of the tuberous sclerosis gene on chromosome 16. *Cell* 1993;75:1305–1315. [PubMed: 8269512]
2. van Slegtenhorst M, et al. Identification of the tuberous sclerosis gene *TSC1* on chromosome 9q34. *Science* 1997;277:805–808. [PubMed: 9242607]
3. Joinson C, et al. Learning disability and epilepsy in an epidemiological sample of individuals with tuberous sclerosis complex. *Psychol Med* 2003;33:335–344. [PubMed: 12622312]

4. de Vries PJ, Prather PA. The tuberous sclerosis complex. *N Engl J Med* 2007;356:92. [PubMed: 17202464]author reply 93–94
5. de Vries PJ, Howe CJ. The tuberous sclerosis complex proteins—a GRIPP on cognition and neurodevelopment. *Trends Mol Med* 2007;13:319–326. [PubMed: 17632034]
6. Harrison JE, O’Callaghan FJ, Hancock E, Osborne JP, Bolton PF. Cognitive deficits in normally intelligent patients with tuberous sclerosis. *Am J Med Genet* 1999;88:642–646. [PubMed: 10581483]
7. Ridler K, et al. Neuroanatomical correlates of memory deficits in tuberous sclerosis complex. *Cereb Cortex* 2007;17:261–271. [PubMed: 16603714]
8. Onda H, Lueck A, Marks PW, Warren HB, Kwiatkowski DJ. *Tsc2*^{+/-} mice develop tumors in multiple sites that express gelsolin and are influenced by genetic background. *J Clin Invest* 1999;104:687–695. [PubMed: 10491404]
9. Waltereit R, et al. Enhanced episodic-like memory and kindling epilepsy in a rat model of tuberous sclerosis. *J Neurochem* 2006;96:407–413. [PubMed: 16300636]
10. von der Brelie C, Waltereit R, Zhang L, Beck H, Kirschstein T. Impaired synaptic plasticity in a rat model of tuberous sclerosis. *Eur J Neurosci* 2006;23:686–692. [PubMed: 16487150]
11. Goorden SM, van Woerden GM, van der Weerd L, Cheadle JP, Elgersma Y. Cognitive deficits in *Tsc1*^{+/-} mice in the absence of cerebral lesions and seizures. *Ann Neurol* 2007;62:648–655. [PubMed: 18067135]
12. Murthy V, et al. Developmental expression of the tuberous sclerosis proteins tuberin and hamartin. *Acta Neuropathol* 2001;101:202–210. [PubMed: 11307618]
13. Floresco SB, Seamans JK, Phillips AG. Selective roles for hippocampal, prefrontal cortical and ventral striatal circuits in radial-arm maze tasks with or without a delay. *J Neurosci* 1997;17:1880–1890. [PubMed: 9030646]
14. Olton D, Becker J, Handelmann G. Hippocampus, space and memory. *Behav Brain Sci* 1979;2:313–365.
15. Frankland PW, Cestari V, Filipkowski RK, McDonald RJ, Silva AJ. The dorsal hippocampus is essential for context discrimination but not for contextual conditioning. *Behav Neurosci* 1998;112:863–874. [PubMed: 9733192]
16. Sancak O, et al. Mutational analysis of the *TSC1* and *TSC2* genes in a diagnostic setting: genotype-phenotype correlations and comparison of diagnostic DNA techniques in tuberous sclerosis complex. *Eur J Hum Genet* 2005;13:731–741. [PubMed: 15798777]
17. Kwiatkowski DJ, Manning BD. Tuberous sclerosis: a GAP at the crossroads of multiple signaling pathways. *Hum Mol Genet* 2005;14:R251–R258. [PubMed: 16244323]
18. Tang SJ, et al. A rapamycin-sensitive signaling pathway contributes to long-term synaptic plasticity in the hippocampus. *Proc Natl Acad Sci USA* 2002;99:467–472. [PubMed: 11756682]
19. Kwiatkowski DJ, et al. A mouse model of *TSC1* reveals sex-dependent lethality from liver hemangiomas and up-regulation of p70S6 kinase activity in *Tsc1* null cells. *Hum Mol Genet* 2002;11:525–534. [PubMed: 11875047]
20. Dragatsis I, Zeitlin S. CaMKI α -Cre transgene expression and recombination patterns in the mouse brain. *Genesis* 2000;26:133–135. [PubMed: 10686608]
21. Kwon CH, Zhu X, Zhang J, Baker SJ. mTor is required for hypertrophy of *Pten*-deficient neuronal soma *in vivo*. *Proc Natl Acad Sci USA* 2003;100:12923–12928. [PubMed: 14534328]
22. Lewis JC, Thomas HV, Murphy KC, Sampson JR. Genotype and psychological phenotype in tuberous sclerosis. *J Med Genet* 2004;41:203–207. [PubMed: 14985384]
23. O’Callaghan FJ, et al. The relation of infantile spasms, tubers and intelligence in tuberous sclerosis complex. *Arch Dis Child* 2004;89:530–533. [PubMed: 15155396]
24. Raznahan A, et al. Biological markers of intellectual disability in tuberous sclerosis. *Psychol Med* 2007;37:1293–1304. [PubMed: 17335641]
25. Jaworski J, Sheng M. The growing role of mTOR in neuronal development and plasticity. *Mol Neurobiol* 2006;34:205–219. [PubMed: 17308353]
26. Tavazoie SF, Alvarez VA, Ridenour DA, Kwiatkowski DJ, Sabatini BL. Regulation of neuronal morphology and function by the tumor suppressors *Tsc1* and *Tsc2*. *Nat Neurosci* 2005;8:1727–1734. [PubMed: 16286931]

27. Banko JL, et al. The translation repressor 4E-BP2 is critical for eIF4F complex formation, synaptic plasticity, and memory in the hippocampus. *J Neurosci* 2005;25:9581–9590. [PubMed: 16237163]
28. Dash PK, Orsi SA, Moore AN. Spatial memory formation and memory-enhancing effect of glucose involves activation of the tuberous sclerosis complex–Mammalian target of rapamycin pathway. *J Neurosci* 2006;26:8048–8056. [PubMed: 16885218]
29. Vanderklish PW, Edelman GM. Differential translation and fragile X syndrome. *Genes Brain Behav* 2005;4:360–384. [PubMed: 16098135]
30. Bear MF, Dolen G, Osterweil E, Nagarajan N. Fragile X: translation in action. *Neuropsychopharmacology* 2008;33:84–87. [PubMed: 17940551]

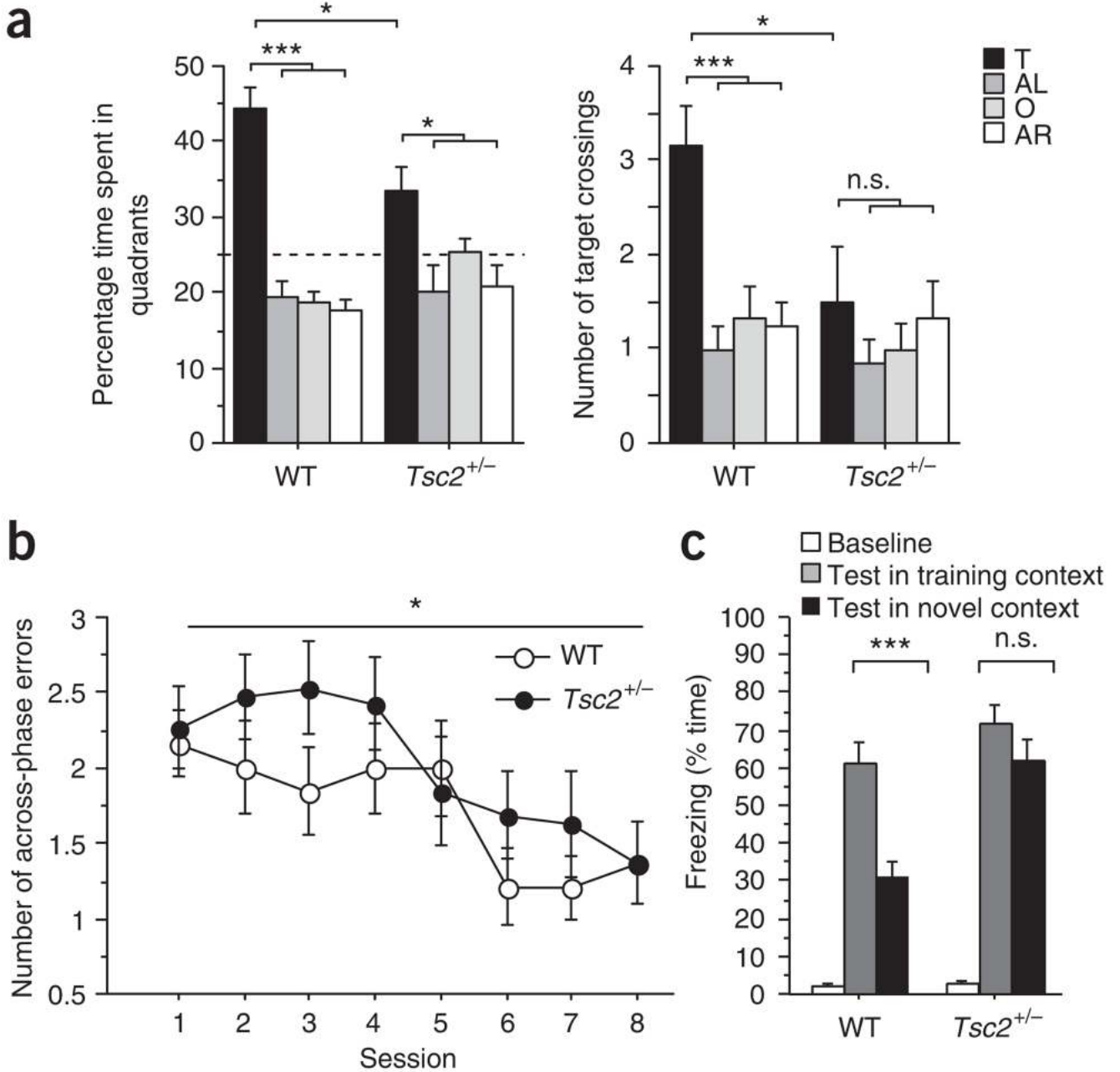
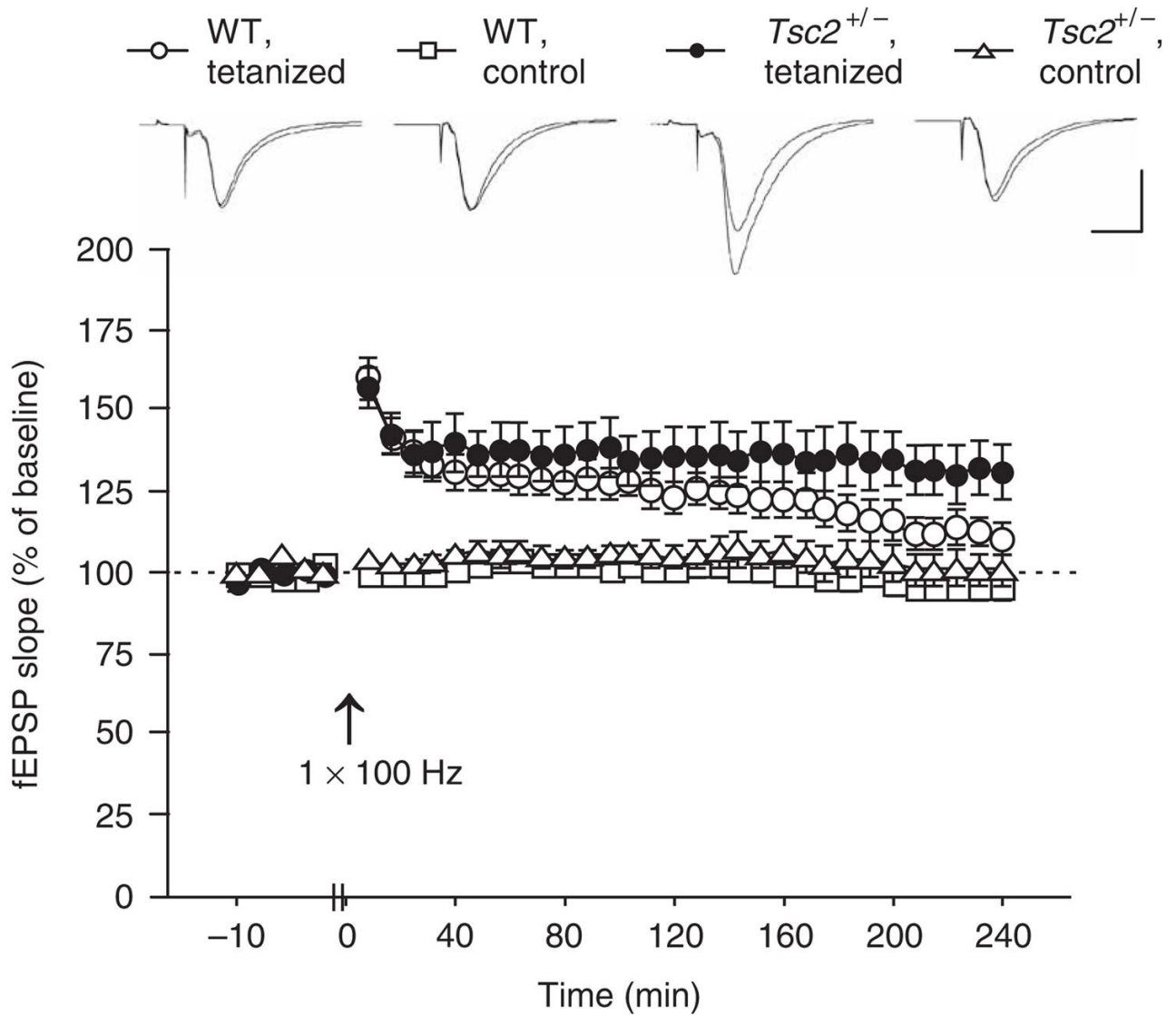


Figure 1. *Tsc2*^{+/-} mice show learning deficits in three hippocampus-dependent tasks. **(a)** Quadrant occupancy and target crossings during the probe trial given after completion of Morris water maze training ($n = 12$ mice per genotype; two-way ANOVA for quadrant occupancy with genotype as between-subjects factor and pool quadrant as within-subjects factor, genotype \times pool quadrant interaction: $F(3,88) = 4.763$, $P = 0.004$; two-way ANOVA for target crossings with genotype as between-subjects factor and pool quadrant as within-subjects factor, effect of genotype: $F(1,88) = 4.278$, $P = 0.0415$). Pool quadrants: target quadrant (T), adjacent right (AR), adjacent left (AL), opposite quadrant (O). Dashed line marks chance performance in the Morris water maze. **(b)** Number of across-phase errors in eight-arm radial maze plotted against training session ($n = 19$ mice per genotype; one-way repeated-measures ANOVA with

genotype as between-subjects factor: $F(1,36) = 4.724$, $P = 0.0364$). (c) Context discrimination: freezing scores before shock (baseline) and during the test in the training context (WT mice: $n = 11$ mice; $Tsc2^{+/-}$ mice: $n = 9$ mice) or the novel context (WT mice: $n = 10$ mice; $Tsc2^{+/-}$ mice: $n = 9$ mice). * $P < 0.05$, *** $P < 0.001$, n.s., not significant ($P > 0.05$). Data represent means \pm s.e.m.

**Figure 2.**

An E-LTP stimulation paradigm elicited L-LTP in *Tsc2*^{+/-} mice. Initial fEPSP slopes recorded from hippocampal slices are shown before (baseline) and following LTP induction (with a 1-s, 100-Hz tetanus) for the tetanized pathway and for a separate, untetanized pathway (control). Data are plotted in 2-min blocks for baseline and 8-min blocks for time after LTP induction (WT slices, $n = 9$ slices from 9 mice; *Tsc2*^{+/-} slices, $n = 7$ slices from 7 mice; one-way repeated-measures ANOVA with genotype as between-subjects factor, measure \times genotype interaction: $F(29,406) = 2.436$, $P < 0.0001$; t -test, last 10 min of recording, $P = 0.0328$). Sample traces show responses (ten responses were averaged) during baseline and the last 10 min of recording, respectively. Scale: vertical bar, 1 mV; horizontal bar, 10 ms. Data represent means \pm s.e.m.

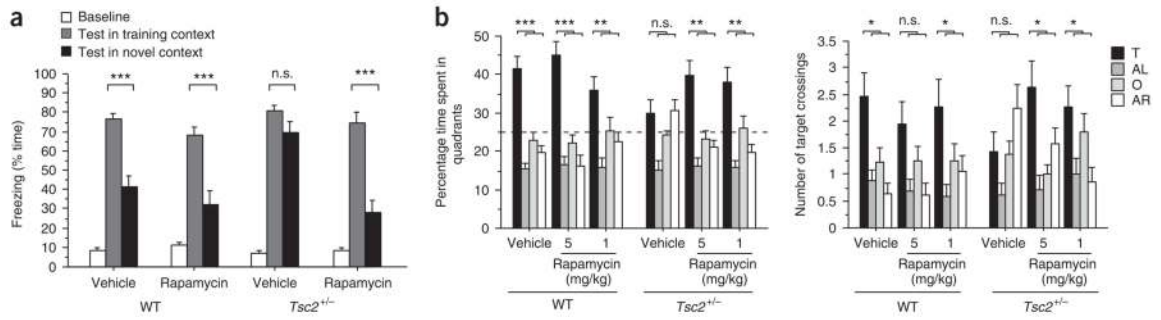


Figure 3.

Rapamycin reversed context discrimination and spatial learning deficits in *Tsc2*^{+/-} mice. **(a)** Context discrimination: freezing scores before shock (baseline) and during the test in the training context (vehicle-treated WT mice, *n* = 12; rapamycin-treated WT mice, *n* = 13; vehicle-treated *Tsc2*^{+/-} mice, *n* = 9; rapamycin-treated *Tsc2*^{+/-} mice, *n* = 9) or the novel context (vehicle-treated WT mice, *n* = 12; rapamycin-treated WT mice, *n* = 12; vehicle-treated *Tsc2*^{+/-} mice, *n* = 10; rapamycin-treated *Tsc2*^{+/-} mice, *n* = 11). **(b)** Quadrant occupancy and target crossings during the probe trial that was given after completion of Morris water maze training (vehicle-treated WT mice, *n* = 17; WT mice treated with 1 mg/kg rapamycin, *n* = 15; WT mice treated with 5 mg/kg rapamycin, *n* = 16; vehicle-treated *Tsc2*^{+/-} mice, *n* = 16; *Tsc2*^{+/-} mice treated with 1 mg/kg rapamycin, *n* = 15; *Tsc2*^{+/-} mice treated with 5 mg/kg rapamycin, *n* = 14; three-way ANOVA for quadrant occupancy with genotype and treatment as between-subjects factors and pool quadrant as within-subjects factor, genotype × treatment × quadrant interaction: $F(6,348) = 2.168$, $P = 0.0456$; three-way ANOVA for target crossings with genotype and treatment as between-subjects factors and pool quadrant as within-subjects factor, genotype × treatment × quadrant interaction: $F(6,348) = 2.908$, $P = 0.0088$). Dashed line marks chance performance in the Morris water maze. * $P < 0.05$, ** $P < 0.01$, *** $P < 0.001$. Data represent means ± s.e.m.

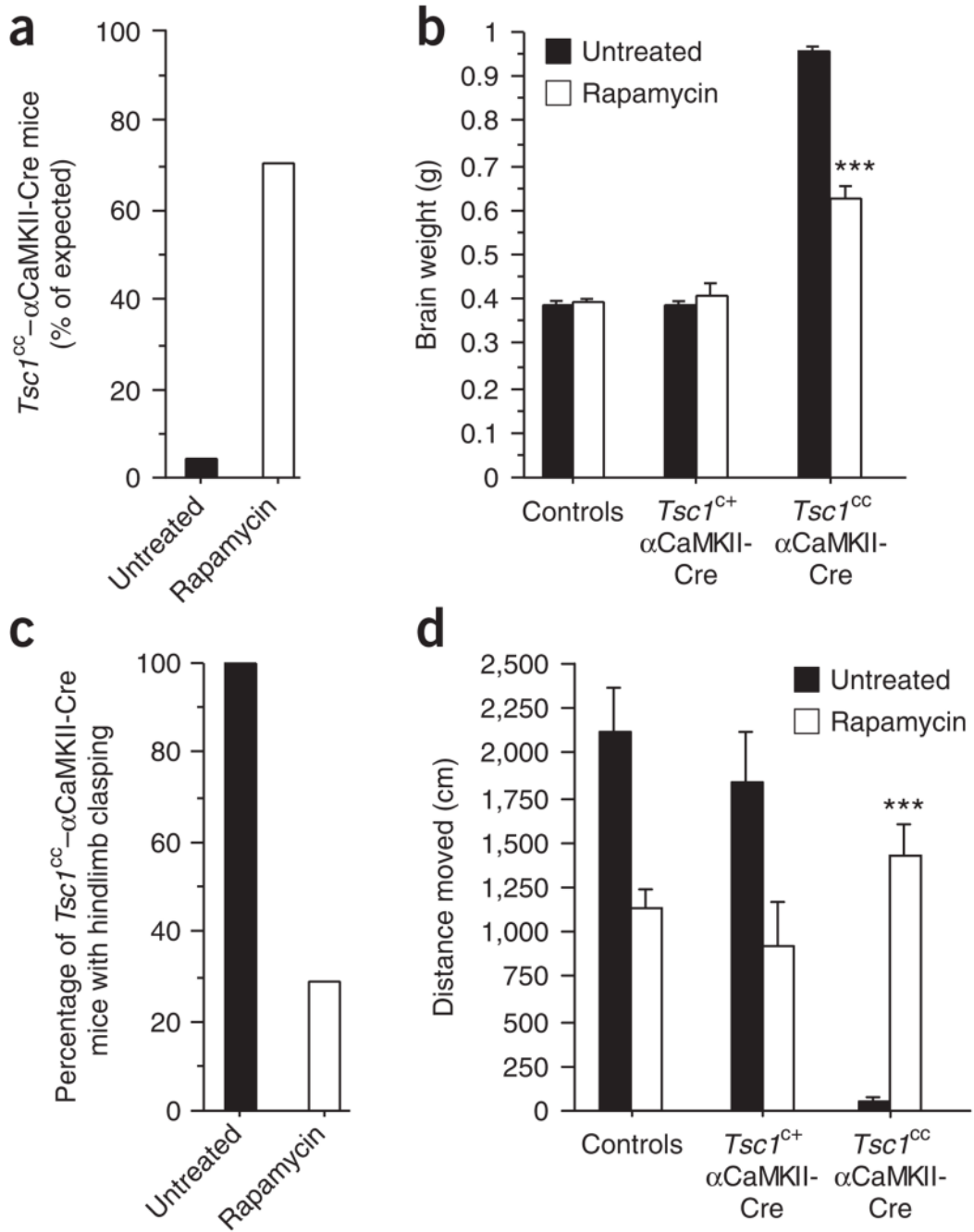


Figure 4. Rapamycin treatment rescues lethality, reduces abnormal brain enlargement and improves neurological findings in *Tsc1^{cc}-αCaMKII-Cre* mice. **(a)** Percentage of untreated and rapamycin-treated *Tsc1^{cc}-αCaMKII-Cre* mice that survived to the age of three months. **(b)** Brain weight at the age of 3 months (untreated *Tsc1^{cc}-αCaMKII-Cre* mice, *n* = 3 mice; rapamycin-treated *Tsc1^{cc}-αCaMKII-Cre* mice, *n* = 4 mice; *t*-test, *P* < 0.001). **(c)** Percentage of untreated and rapamycin-treated *Tsc1^{cc}-αCaMKII-Cre* mice that showed a pathological hindlimb clasping reflex at the age of 3 months. **(d)** Ambulatory distance in the open field assessed at the age of 3 months (untreated *Tsc1^{cc}-αCaMKII-Cre* mice, *n* = 3 mice; rapamycin-

treated *Tsc1^{cc}-αCaMKII-Cre* mice, $n = 7$ mice; t -test, $P < 0.001$). *** $P < 0.001$. Data represent means \pm s.e.m.